Inorganic Chemistry

Article

pubs.acs.org/IC

Sulfinato Iron(III) Complex for Electrocatalytic Proton Reduction

Andrew C. Cavell,[†] Carolyn L. Hartley,[†] Dan Liu,[†] Connor S. Tribble,[†] and William R. McNamara*[,†]

[†]Department of Chemistry, College of William and Mary, 540 Landrum Drive, Williamsburg, Virginia 23185, United States

Supporting Information

ABSTRACT: We report the first example of a sulfinato Fe(III) complex acting as a highly active electrocatalyst for proton reduction. The sulfinate binds to the metal through oxygen, resulting in a seven-membered chelate ring that is likely hemilabile during catalysis. Proton reduction occurs at −1.57 V versus Fc/Fc^+ in CH_3CN with an i_c/i_p = 13 in CH_3CN (k_{obs} = 3300 s^{-1}) and an overpotential of 800 mV. The catalysis is first order with respect to [catalyst] and second order with respect to [trifluoracetic acid]. An 11% increase in catalytic activity is observed in the presence of water, suggesting that sulfinate moieties are viable functional groups for aqueous proton reduction catalysts.

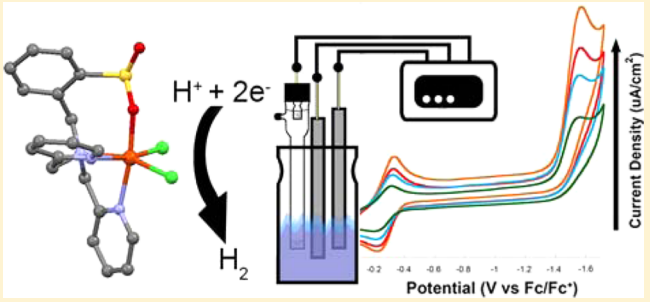

INTRODUCTION

With dwindling fossil fuel reserves and rising greenhouse gas emissions, the development and use of renewable energy sources is critical.[1] Using photons to split water into O_2 and H_2 provides a promising method of harvesting solar energy. To fully realize this goal, proton reduction catalysts must be developed that are made from earth-abundant materials.[1] Since iron is the most abundant transition metal, it is of interest to explore the use of iron in complexes that are highly active and stable for hydrogen generation catalysis.

Other first row transition metals such as Co and Ni have been studied extensively for use as proton reduction catalysts.[2] In the pursuit of improved stability, pentadentate polypyridyl ligands have been used to form complexes that generate hydrogen from aqueous solutions.[3] Although cobalt and nickel complexes are widely studied, few iron catalysts have been examined that both operate at modest potentials and are highly active for proton reduction. To this end, there have been many efforts to mimic the active site of hydrogenase enzymes.[4] There are other recent examples of iron catalysts that are only active in nonaqueous media.[5] Notably, there have also been recent advances in using iron complexes as catalysts for electrocatalytic H_2 oxidation.[6] However, examples of iron-containing proton reduction catalysts that are stable in aqueous media are more limited and do not yet approach the activity of Ni or Co catalysts.[7]

Recently, we reported a mononuclear iron complex (**1**) containing a polypyridyl monophenolate ligand that was stable in aqueous solution and generated hydrogen in CH_3CN with a k_{obs} = 1000 s^{-1}.[8] The mechanism involves protonation of the phenolate prior to subsequent protonation and reduction events (CECE or CEEC). We reasoned that if the dissociation of the protonated phenolate was involved in the rate-limiting step, replacing the phenolate with a functionality that formed a less favorable chelate ring would improve the activity of the catalyst. Herein we report a sulfinato Fe(III) polypyridyl complex (**2**) that forms a seven-membered chelate ring with Fe(III) (Figure 1). This complex is significantly more active

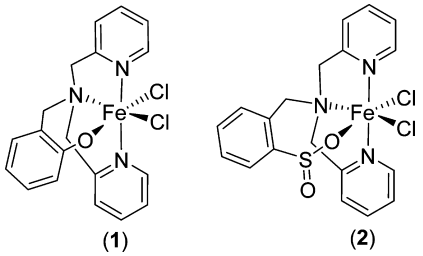

Figure 1. (left) Iron polypyridyl monophenolate complex (**1**). (right) Iron polypyridyl sulfinate complex (**2**).

than the phenolate catalyst for proton reduction with an i_c/i_p = 13 (k_{obs} = 3300 s^{-1}), where i_c is the catalytic current and i_p is the peak current of the complex when no acid is added (see Supporting Information).

Fe(II) and Fe(III) sulfinate complexes have been of great interest in the development of structural mimics of cysteine dioxygenase (CDO).[9] CDO utilizes the S-oxygenation of cysteine, which is crucial for the biosynthesis of pyruvate and taurine.[9] To date, very few CDO mimics have been reported that make use of O_2 as the oxidant.[9,10] Fe sulfinate complexes are typically synthesized by reacting the thiolate complex with pure O_2, resulting in S-oxygenation to give the sulfinate product.[9] However, in obtaining the desired complex **2**, S-oxygenation occurs rapidly in air. Owing to rapid S-oxygenation, efforts to isolate the pure thiolate complex in our

Received: December 18, 2014
Published: March 25, 2015

 © 2015 American Chemical Society

DOI: 10.1021/ic5030394
Inorg. Chem. 2015, 54, 3325−3330

laboratory have been unsuccessful using standard Schlenk techniques (Scheme 1).

Scheme 1. Synthesis of 2

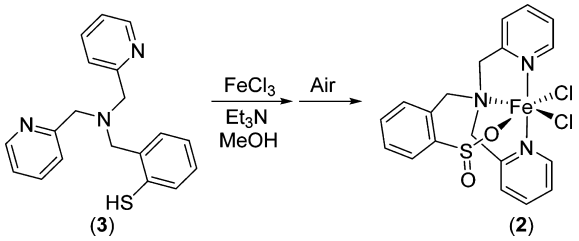

RESULTS AND DISCUSSION

The ligand was synthesized using a modified literature procedure to give **3** in moderate yield (45%). The free ligand (**3**) is stable in air with no ligand oxidation observed after several weeks. The sulfinate complex (**2**) was then obtained by deprotonating the thiolate ligand (**3**) using triethylamine and treating the solution with $FeCl_3$ in a methanol solution under argon. The resulting complex was recrystallized from dichloromethane and then ethanol to give the pure product as a brown solid. X-ray quality crystals were obtained through slow diffusion of diethyl ether through acetonitrile.

The structure confirms that the sulfinato complex (**2**) is coordinated through the oxygen of the sulfinate resulting in a seven-membered chelate ring (Figure 2). The structure shows a

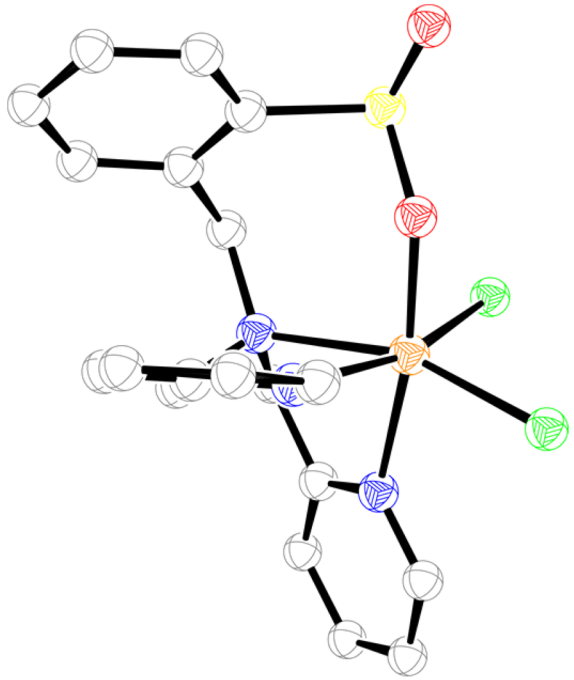

Figure 2. ORTEP diagram of **2**. Ellipsoids are at the 50% probability level with hydrogen omitted for clarity.

distorted octahedral complex with O−Fe−N and N−Fe−Cl bond angles of 170.22° and 161.41°, respectively. The Fe−O for the sulfinato group is 1.934 Å and is longer than what was reported for the Fe−O of the phenolate complex (**1**). The S−O bond lengths of 1.451 and 1.527 Å are consistent with a double bond to the unbound oxygen and a single bond to the oxygen that is coordinated to iron.

Cyclic voltammograms (CVs) of the complex (**2**) in acetonitrile reveal a reversible redox couple for Fe(II/III) at −0.28 V versus Fc/Fc^+. A peak separation of 70 mV is observed under these conditions, which is consistent with the peak separation observed for the Fc/Fc^+ redox couple under the same conditions. With the addition of known concentrations of trifluoracetic acid (TFA) in acetonitrile, an irreversible reduction event is observed at −1.57 V versus Fc/Fc^+. Calculations using the catalytic half-wave potential and the E_{ref} for TFA in acetonitrile indicate that the catalysis occurs with an 800 mV overpotential.[11] When more acid is added, a larger current enhancement is observed (Figure 3).

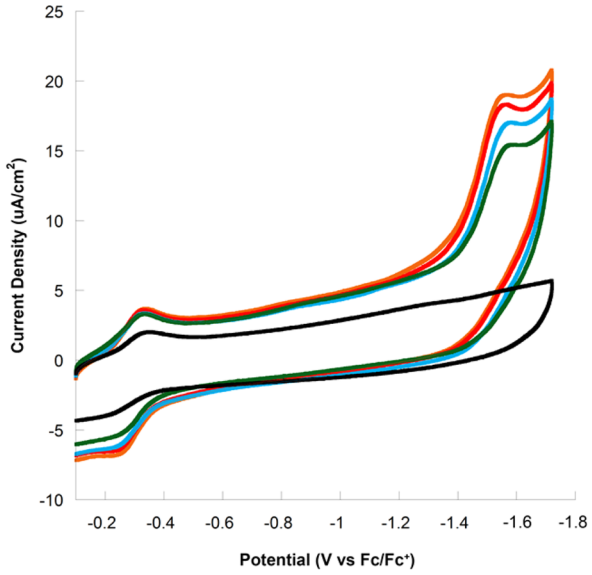

Figure 3. CVs of **2** in CH_3CN with 0.1 M $TBAPF_6$ (black) upon addition of 2.2 mM (green), 4.4 mM (blue), 6.6 mM (red), and 8.8 mM (orange) TFA at ν = 200 mV/s.

The linear relationship between i_c and [TFA] suggests a second-order dependence on proton concentration (see Supporting Information). The catalyst is highly active for proton reduction with an i_c/i_p = 13, corresponding to a k_{obs} = 3300 s^{-1} (see Supporting Information). Although the method used to calculate k_{obs} accurately represents simple pseudo-first-order systems, it is also used to determine turnover frequencies (TOFs) for more complicated systems to provide a point of comparison for different catalysts.[3a,c,12] This compares favorably with other iron complexes in the literature.[5,7] Complex **2** is also significantly more active than the phenolate complex (**1**), which gave an i_c/i_p = 7.8 under identical conditions, corresponding to a k_{obs} = 1000 s^{-1}.

Furthermore, when [TFA] is held constant and catalyst is introduced, a catalytic wave is also observed at −1.57 V. Addition of more catalyst then results in a larger current enhancement (Figure 4). After several additions of **2** there is a linear relationship between [catalyst] and i_c/i_p. This suggests that there is a first-order dependence on [catalyst], resulting in an overall rate expression of rate = $k[\mathbf{2}][H^+]^2$.

When acid is added to the phenolate complex (**1**) the redox couple for Fe(II)/Fe(III) shifts from −0.6 to −0.3 V versus Fc/Fc^+ (Figure 5, right).[8] The shift in redox couple suggests that a new complex is formed upon addition of acid. Owing to the fact

DOI: 10.1021/ic5030394
Inorg. Chem. 2015, 54, 3325−3330

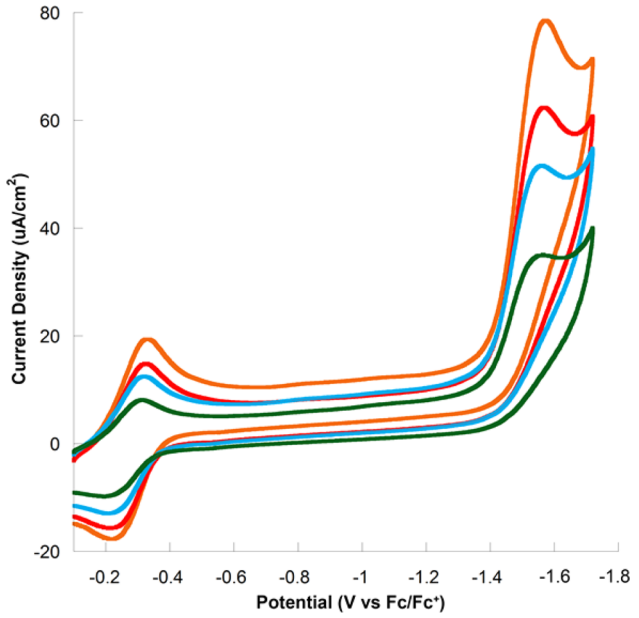

Figure 4. CVs in CH_3CN with 0.1 M $TBAPF_6$ containing 44 mM TFA with 0.2 mM **2** (green), 0.4 mM **2** (blue), 0.6 mM **2** (red), and 0.8 mM **2** at ν = 200 mV/s.

that the most basic site of the complex is the phenolate, the first step in the catalytic cycle involves protonation of the oxygen. In contrast, upon addition of TFA, the redox couple for Fe(II)/Fe(III) does not shift for complex **2** (Figure 5, left), indicating that this catalyst operates under a different mechanism. With no observed shift in the redox couple, the first step is proposed to involve an electrochemical reduction, which is followed by protonation and reduction events (ECEC or ECCE). It is also possible that catalysis occurs through a more complicated mechanism than what can be deduced from electrochemical analysis alone.

Upon addition of TFA, the onset of the catalytic wave is observed at the same potential for both complexes **1** and **2**. This suggests that both ligands are hemilabile in nature, leaving the same Fe-NNN core intact during later stages of the catalytic cycle. The phenolate in complex **1** is first protonated and becomes labile upon reduction. The sulfinate group of complex **2** forms a less-favored seven-membered chelate ring, increasing the lability of this site. The resulting difference in catalytic activity of **1** and **2** indicates that the dissociation of the phenol group in complex **1** is likely involved in the slow step of the catalytic cycle. Therefore, by replacing it with a more labile sulfinate group, a significant increase in rate is observed.

With many iron catalysts operating at more cathodic potentials, it is crucial to choose a proton source that is not reduced at these potentials. Figure 6 shows that the background reduction of [TFA] does not contribute significantly to the value of i_c/i_p.[13] Although homoconjugation is observed for TFA, the lack of background reduction at −1.57 V versus Fc/Fc^+ makes it viable for studying this complex.

Since it is of great interest to develop catalysts that can reduce protons in aqueous solutions, it is also important to determine if **2** is active in the presence of water. Figure 7 shows the CVs of **2** in CH_3CN with 11 mM TFA added (green). Upon addition of 100 μL (1.1 M) of water, an increase in catalytic activity is observed (blue). This increase corresponds to an 11% improvement in catalytic performance for **2** with water present. The increase in activity suggests that the unbound sulfinate is stabilized by the presence of a polar, protic solvent such as water. At high concentrations of water, the complex does not decompose but is sparingly soluble. Owing to solubility issues, we could not perform an experiment in 1:1 CH_3CN/H_2O to directly compare **1** and **2** in aqueous environments. Solubility also limited our ability to test the activity of **2** in purely aqueous buffered solutions. However, the increase in i_c/i_p observed with water added suggests that water-soluble catalysts with sulfinato moieties have the potential to be highly active in aqueous solutions.

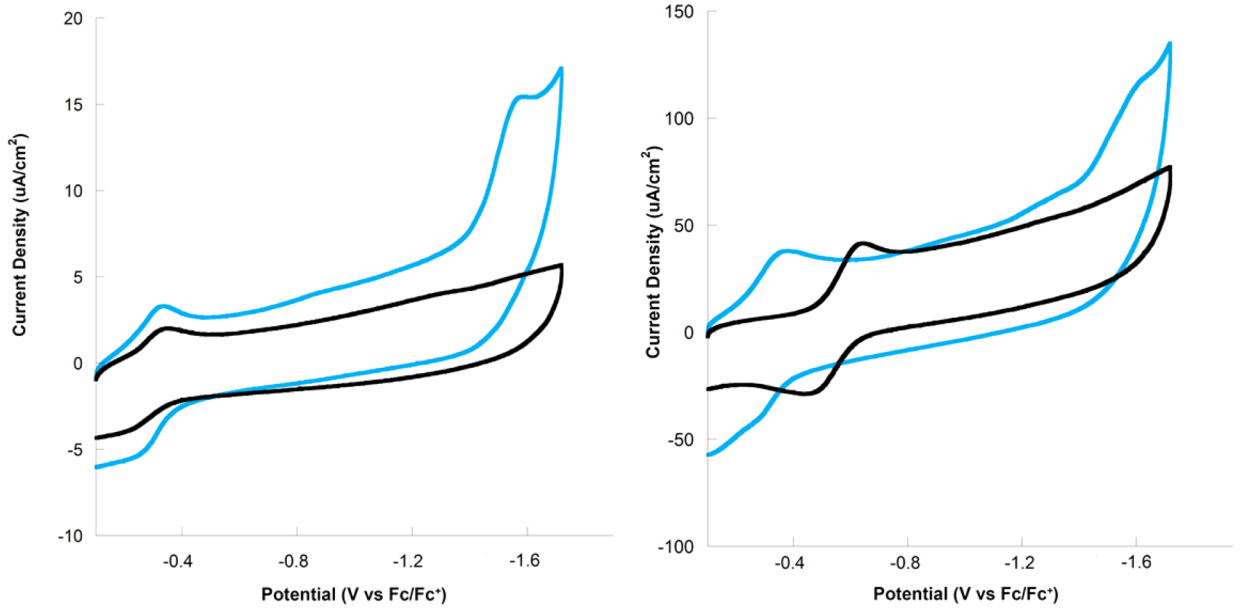

Figure 5. (left) CVs of **2** without added TFA (black) and with 8.8 mM TFA (blue). (right) CVs of **1** without added TFA (black) and with 8.8 mM TFA (blue).

DOI: 10.1021/ic5030394
Inorg. Chem. 2015, 54, 3325−3330

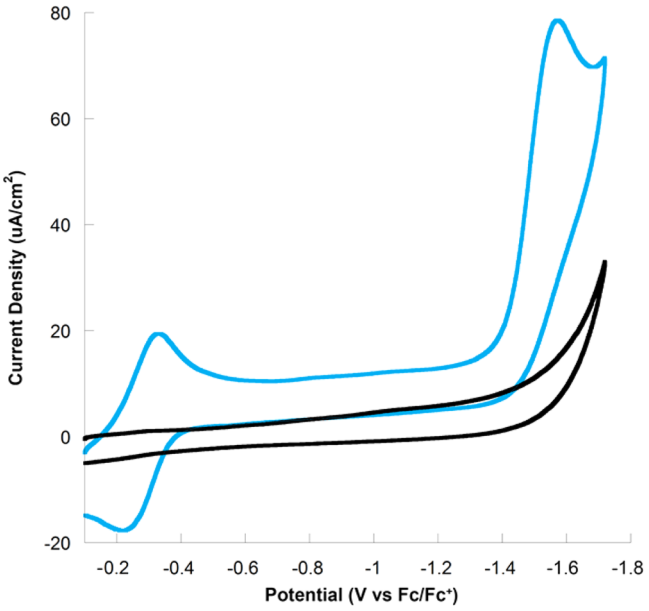

Figure 6. CVs of 22 mM TFA in 0.1 M $TBAPF_6$ in CH_3CN prior to (black) and after (blue) the addition of 0.5 mM **2** at ν = 200 mV/s. A reduction peak corresponding to the catalytic reduction of hydrogen is visible at −1.57 V only upon addition of **2**.

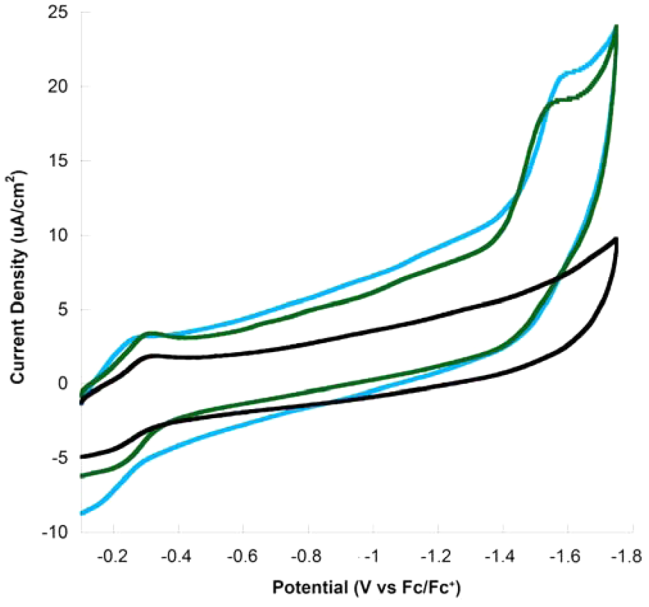

Figure 7. CVs of **2** in a CH_3CN solution with 0.1 M $TBAPF_6$ and 11 mM TFA in dry conditions (green) and upon addition of 100 μL (1.1 M) of water (blue) at ν = 200 mV/s. The black trace represents the CV of **2** in CH_3CN with no acid added.

CONCLUSION

In conclusion, an iron complex with a sulfinato moiety has been found to be highly active for electrocatalytic proton reduction. It is the first example of a sulfinato Fe(III) complex that is an active catalyst for this reaction. The sulfinate binds to the metal through oxygen, resulting in a seven-membered chelate ring. The catalyst reduces protons at −1.57 V versus Fc/Fc^+ (800 mV overpotential) with an i_c/i_p = 13, making it significantly more active (k_{obs} = 3300 s^{-1}) than the previously reported phenolate complex (**1**). This higher activity is likely a result of the hemilabile nature of the ligand due to the presence of the seven-membered chelate ring. The catalysis is first order with respect to [catalyst] and second order with respect to [TFA]. It is also active in the presence of water with an increase in activity observed after the addition of 100 μL (1.1 M) H_2O. The incorporation of a sulfinate moiety has resulted in the development of a more active iron catalyst and has helped to elucidate the mechanism of the previously reported iron phenolate catalyst.

EXPERIMENTAL SECTION

Materials. All experiments were performed using standard Schlenk air-free techniques under an Ar atmosphere unless otherwise indicated. All chemicals were purchased from Fischer Scientific and were used without further purification unless noted otherwise.

Instrumentation. ^1H and ^{13}C spectra were recorded on an Agilent 400MR DD2 spectrometer operating in the pulse Fourier transform mode. Chemical shifts are referenced to residual solvent. Elemental analysis was carried out by the CENTC Elemental Analysis Facility at the University of Rochester, funded by NSF CHE-0650456. UV−vis spectra were recorded using an Agilent Cary 60 UV−vis Spectrophotometer using air-free solutions in sealed quartz cuvettes. All electrochemical experiments were performed under an atmosphere of Ar using a CH Instruments 620D potentiostat. CVs were acquired using a standard three-electrode cell. Prior to each acquisition, the working electrode (glassy carbon) and the auxiliary electrode (platinum) were polished using 0.05 μm alumina powder paste on a cloth-covered polishing pad, followed by rinsing with water and acetonitrile. The reference used was a saturated calomel electrode (SCE) electrode unless otherwise noted. Ferrocene was used as an internal standard to correct for drifting of the reference electrode and changes in concentration, and all potentials are reported relative to the ferrocene/ferrocenium (Fc/Fc^+) redox couple. Controlled potential coulometry was carried out in a sealed 500 mL cell using vitreous carbon working and counter electrodes and a Ag wire reference electrode separated by porous VYCOR frits. A CH Instruments 620D potentiostat combined with a CH Instruments 680 A booster was used for the CPC. Gas analysis for H_2 was performed using a Bruker Scion 436 gas chromatograph equipped with a TCD using Ar carrier gas and calibrated with H_2/CH_4 gas mixtures of known composition.

X-ray Diffractometry. Single crystals were mounted on glass fibers. All data for **2** were collected using graphite-monochromated Mo Kα radiation on a Bruker SMART Apex II CCD platform diffractometer. The structure was solved using SIR20114 and refined using SHELXL-2014/7. The space group $P4_3$ was determined based on CSD statistics and having solved the structure in space groups $P1$ and $P2_1$ and noting the higher symmetry visually and via the Addsym function of program Platon. Systematic absences clearly chose $P4_2$; however, no solution was obtainable in that space group. A solution in space group $P2_1$ that included modeling for pseudomerohedral twinning also did not produce a better result than that obtained in $P4_3$. A direct-methods solution was calculated, which provided most non-hydrogen atoms from the E-map. Full-matrix least-squares/difference Fourier cycles were performed, which located the remaining non-hydrogen atoms. All non-hydrogen atoms were refined with anisotropic displacement parameters. All hydrogen atoms were placed in ideal positions and refined as riding atoms with relative isotropic displacement parameters.

Reflection contributions from highly disordered solvent, located in channels along the crystallographic 4_3 axes at the corners of the unit cell, were fixed and added to the calculated structure factors using the Squeeze routine of program Platon, which determined there to be 68 electrons in 212 $Å^3$ removed per unit cell.

Syntheses. The ligand (**3**) was synthesized from thiosalicylic acid using a modified literature procedure.[14]

***o*-Mercaptobenzyl Alcohol.** Thiosalicylic acid (3.0908 g, 0.02 mol) in 75 mL of **dry** diethyl ether was degassed with Ar. This was combined with $LiAlH_4$ (1.1385 g, 0.03 mol) under air-free conditions, and the solution was stirred at room temperature for 1 h. The solution was cooled in an ice bath, and 4 mL H_2O was added dropwise,

DOI: 10.1021/ic5030394
Inorg. Chem. 2015, 54, 3325−3330

followed by 20 mL of 10% H_2SO_4. The solution was then allowed to stir under argon for 48 h. The reaction mixture was washed with diethyl ether (3 × 30 mL), and the organic layer was dried using $MgSO_4$ and evaporated to yield *o*-mercaptobenzyl alcohol, a yellow oil. (82% yield) The ^1H and ^{13}C NMR spectra matched reported values.[14]

3-(2-Hydroxymethylphenylsulfanyl)propionitrile. A solution of *o*-mercaptobenzyl alcohol (0.9974 g, 7.12 mmol) in 15 mL of ethanol was prepared and degassed. This was combined with a degassed solution of NaOH (0.4058 g, 0.01 mol) in 5 mL of H_2O and 10 mL of ethanol. Degassed bromopropionitrile (0.6 mL, 7.1 mmol) was added dropwise under air-free conditions, and the mixture was allowed to stir at room temperature for 5 h. The resulting solution was filtered and evaporated to yield an oily yellow solution. This was dissolved in 25 mL of diethyl ether, washed with 10 mL of 5% NaOH and 10 mL of H_2O, then dried with $MgSO_4$ and evaporated to yield a white solid, 3-(2-hydroxymethylphenylsulfanyl)propionitrile. The ^1H and ^{13}C NMR spectra matched reported values.[14]

3-(2-Bromomethylphenylsulfanyl)propionitrile. Solid 3-(2-hydroxymethylphenylsulfanyl)propionitrile (0.2739 g, 1.473 mmol) was dissolved in 22 mL of dichloromethane and degassed with argon. This was added to a Schlenk flask under air-free conditions, and the reaction was cooled in an ice bath. 1.0 M PBr_3 (0.6 mL, 0.6 mmol) was added dropwise to the Schlenk, and the solution was allowed to stir for 4 h. The clear yellow-orange solution was washed with 10 mL of 10% NaOH and 10 mL of H_2O, dried with $MgSO_4$, filtered, and evaporated to yield 3-(2-bromomethylphenylsulfanyl)propionitrile as a clear yellow oil (80% yield). The ^1H and ^{13}C NMR spectra matched reported values.[14]

***N*-(2-Propionitilemercaptobenzyl)-*N*,*N*-bis(2-pyridylmethyl)-amine.** 3-(2-bromomethylphenylsulfanyl)propionitrile (0.347 g, 1.355 mmol) was dissolved in 20 mL of ethyl acetate and degassed with argon. This was added to an air-free Schlenk flask, followed by the addition of a degassed solution of dipicolylamine (0.3 mL, 1.671 mmol) in 15 mL of ethyl acetate, and then a degassed solution of Et_3N (1 mL, 7.17 mmol) in 15 mL of ethyl acetate. This stirred under argon for 72 h. The solution was then filtered and evaporated to yield *N*-(2-propionitrilemercaptobenzyl)-*N*,*N*-bis(2-pyridylmethyl)amine, which was purified through a silica gel column run in 7:3 ethanol/ethyl acetate and collected at 59% yield. The ^1H and ^{13}C NMR spectra matched reported values.[14]

***N*-(2-Mercaptobenzyl)-*N*,*N*-bis(2-pyridylmethyl)amine (3).** *N*-(2-propionitrilemercaptobenzyl)-*N*,*N*-bis(2-pyridylmethyl)amine (40.7 mg, 0.112 mmol) was dissolved in 10 mL of methanol and degassed. The solution was then combined with NaOMe (9.7 mg, 0.180 mmol) in a Schlenk flask under air-free conditions. The solution was refluxed under argon for 72 h. The resulting clear amber colored solution was filtered and evaporated. The resulting solid was dissolved in 13 mL of dichloromethane (DCM) and washed with 13 mL of deionized H_2O to quench the remaining NaOMe. The lower orange-brown organic layer was collected and evaporated to yield a brown oil. The ligand was purified through use of a silica gel column in 9:1 DCM/MeOH. The purified *N*-(2-mercaptobenzyl)-*N*,*N*-bis(2-pyridylmethyl)amine (**3**) was collected at 45% yield as a brown oil. The ^1H and ^{13}C NMR spectra matched reported values.[11] For a representative ^1H NMR spectrum, see Supporting Information, Figure S12. ^1H NMR ($CDCl_3$): ∂ 8.51 (s, 2H), 7.50–7.67 (m, 4H), 7.10–7.37 (m, 7H), 3.87 (s, 2H), 3.80 (s, 4H). High-resolution mass spectrometry (HR MS): m/z for $(C_{19}H_{19}N_3S)H^+$ expected = 322.137 245 m/z found = 322.137 527.

[$FeCl_2$(L-OSO)] (2). The sulfinato Fe(III) complex was synthesized according to the following procedure: **1** (0.100 g, 0.312 mmol) and Et_3N (0.04 mL, 0.312 mmol) were dissolved in 10 mL of MeOH and degassed with Ar. $FeCl_3 \cdot 6H_2O$ (0.843 g, 0.312 mmol) was dissolved in 10 mL of MeOH and degassed with Ar. The two solutions were combined under air-free conditions to yield a brown solution with some visible precipitate. The reaction was stirred at room temperature for 12 h and filtered. The filtrate was evaporated, and the resulting solid was dissolved in DCM to remove impurities through recrystallization. Additional recrystallizations were performed in EtOH. A dark solid of **2** was collected with a 71% yield. Crystals suitable for X-ray diffraction were grown by diffusion of diethyl ether into a concentrated solution of **2** in CH_3CN. HR MS: m/z for $(C_{19}H_{18}Cl_2FeN_3O_2S)Na^+$ expected = 500.973841 m/z found = 500.974354 (see Supporting Information, Figure S14). Anal. Calcd for **2** $FeC_{19}H_{18}Cl_2N_3O_2S$: C, 47.63; H, 3.79; N, 8.77%. Found: C, 47.77; H, 4.12; N, 8.44%. Structure was obtained using X-ray diffraction of a single crystal.

Controlled-Potential Coulometry. Controlled-potential coulometry experiments (CPC) were conducted in a closed 500 mL four-neck round-bottom flask. Complex **2** (0.3 mg, 0.00063 mmol) was added to 50 mL of 0.1 M tetrabutylammonium hexafluorophosphate ($TBAPF_6$) in CH_3CN. The flask was capped with two vitreous carbon electrodes and a silver wire reference electrode, all submerged in the solution and separated by VYCOR frits. The flask was degassed using Ar for 20 min, while the solution was stirred. Using a Hamilton gas syringe, 10 mL of Ar was removed from the flask and replaced with 10 mL of CH_4 for reference. A CV of the solution was then taken from −0.1 to −1.8 V versus Fc/Fc^+ to identify the potential at which proton reduction occurs. A CPC was run at −1.6 V for 1800 s, while the solution continued to stir. Upon completion of the experiment, a 0.10 mL sample of vapor from the flask was removed using a Hamilton gas syringe and injected into a GC. The ratio of H_2 to CH_4 in the sample was compared to a calibration curve to determine the total volume of H_2 produced during the experiment. A faradaic yield of 98% was observed for **2**. No hydrogen was observed when the experiment was run without catalyst.

Catalyst Concentration Dependence. A 5.2 mM stock solution of **2** was prepared by dissolving 0.0125 g of **2** crystals with 0.1 M $TBAPF_6$ in CH_3CN in a 5 mL volumetric flask. A 5 mL solution of 0.1 M $TBAPF_6$ CH_3CN was prepared in an electrochemical cell. 200 μL of 1.1 M TFA (44 mM) was added to the cell, which was degassed with Ar. CVs were taken at 200 mV/s without any catalyst, then in the presence of 0.2, 0.3, 0.4, and 0.5 mM catalyst from the **2** stock solution. CVs were obtained using a glassy carbon working electrode, a Pt auxiliary, and an SCE reference electrode. The working and auxiliary electrodes were polished with 0.05 μm alumina powder paste prior to each acquisition. All i_c values were obtained using the method described in the Supporting Information of this work.

Scan Rate Dependence. In an electrochemical cell, 1.0 mg of **2** (2.09 μmol) was dissolved in 5 mL of CH_3CN with 0.1 M $TBAPF_6$ and degassed with argon. CVs were taken upon addition of 11 mM TFA at various scan rates ranging from 5 to 14 V/s. CVs were obtained using a glassy carbon working electrode, a Pt auxiliary, and an SCE reference electrode. The working and auxiliary electrodes were polished with 0.05 μm alumina powder.

Determination of Overpotential. The tendency of TFA to exhibit homoconjugation in acetonitrile solutions often leads to inaccurate determinations of overpotential if this effect is not taken into account.[11] This renders standard calculations of overpotential using pK_a unreliable.[11] Overpotentials were determined by calculating the difference between the half-wave potential of the catalytic reduction and E_{ref}. E_{ref} refers to a theoretical reduction potential that takes into account the effects of homoconjugation at acid concentrations used in electrochemical experiments.[11b] This method gave overpotential values of ∼800 mV for both TFA and tosic acid.

■ ASSOCIATED CONTENT

Supporting Information

Determination of k_{obs}, sample calculations of k_{obs}, CV data, GC calibration curve, proton concentration study, peak current density versus TFA, scan rate study, dip test study, controlled potential coulometry, $FeCl_3$ control study, UV–vis spectra, tosic acid concentration study, NMR spectrum, HR-MS data, X-ray crystallographic data (including CIF file), ORTEP diagram, and selected bond lengths and angles. This material is available free of charge via the Internet at http://pubs.acs.org.

DOI: 10.1021/ic5030394
Inorg. Chem. 2015, 54, 3325–3330

AUTHOR INFORMATION

Corresponding Author

*E-mail: wrmcnamara@wm.edu.

Notes

The authors declare no competing financial interest.

ACKNOWLEDGMENTS

W.R.M would like to thank R. D. Pike for helpful discussions. W.R.M. would also like to thank W. W. Brennessel and the X-ray crystallography facility at the Univ. of Rochester for solving the crystal structure of **2**. This work was funded by the Virginia Space Grant Consortium New Investigator Award.

REFERENCES

(1) (a) Lewis, N. S.; Nocera, D. G. *Proc. Natl. Acad. Sci. U. S. A.* **2006**, *103*, 15729. (b) Eisenberg, R. *Science* **2009**, *324*, 44.

(2) (a) Connolly, P.; Espenson, J. H. *Inorg. Chem.* **1986**, *25*, 2684. (b) Hu, X.; Brunschwig, B. S.; Peters, J. C. *J. Am. Chem. Soc.* **2007**, *129*, 8988. (c) Dempsey, J. L.; Brunschwig, B. S.; Winkler, J. R.; Gray, H. B. *Acc. Chem. Res.* **2009**, *42*, 1995. (d) Baffert, C.; Artero, V.; Fontecave, M. *Inorg. Chem.* **2007**, *46*, 1817. (e) Razavet, M.; Artero, V.; Fontecave, M. *Inorg. Chem.* **2005**, *44*, 4786. (f) Jacques, P. A.; Artero, V.; Pecaut, J.; Fontecave, M. *Proc. Nat. Acad. Sci. U. S. A.* **2009**, *106*, 20627. (g) Hu, X. L.; Cossairt, B. M.; Brunschwig, B. S.; Lewis, N. S.; Peters, J. C. *Chem. Commun.* **2005**, 4723−4725. (h) DuBois, D. L. *Inorg. Chem.* **2014**, *53*, 3935−3960. (i) Bullock, R. M.; Appel, A. M.; Helm, M. L. *Chem. Commun.* **2014**, *50*, 3125−3143.

(3) (a) Sun, Y.; Bigi, J. P.; Piro, N. A.; Tang, M. L.; Long, J. R.; Chang, C. J. *J. Am. Chem. Soc.* **2011**, *133*, 9212. (b) Bigi, J. P.; Hanna, T. E.; Harman, W. H.; Chang, A.; Chang, C. J. *Chem. Commun.* **2010**, *46*, 958. (c) Sun, Y. J.; Sun, J. W.; Long, J. R.; Yang, P. D.; Chang, C. J. *Chem. Sci.* **2013**, *4*, 118. (d) Karunadasa, H. I.; Chang, C. J.; Long, J. R. *Nature* **2010**, *464*, 1329−1333. (e) Stubbert, B.; Peters, J. C.; Gray, H. B. *J. Am. Chem. Soc.* **2011**, *133*, 9212.

(4) (a) Garcin, E.; Vernede, X.; Hatchikian, E. C.; Volbeda, A.; Frey, M.; Fontecilla-Camps, J. C. *Structure* **1999**, *7*, 557−566. (b) Peters, J. W.; Lanzilotta, W. N.; Lemon, B. J.; Seefeldt, L. C. *Science* **1998**, *282*, 1853−1858. (c) Zhao, X.; Georgakaki, I. P.; Miller, M. L.; Yarbrough, J. C.; Darensbourg, M. Y. *J. Am. Chem. Soc.* **2001**, *123*, 9710−9711. (d) Felton, G. A. N.; Glass, R. S.; Lichtenberger, D. L.; Evans, D. H. *Inorg. Chem.* **2006**, *45*, 9181−9184. (e) Gloaguen, F.; Lawrence, J. D.; Rauchfuss, T. B. *J. Am. Chem. Soc.* **2001**, *123*, 9476−9477. (f) Carroll, M. E.; Barton, B. E.; Rauchfuss, T. B.; Carroll, P. J. *J. Am. Chem. Soc.* **2012**, *134*, 18843−18852.

(5) (a) Kaur-Ghuman, S.; Schwartz, L.; Lomoth, R.; Stein, W.; Ott, S. *Angew. Chem., Int. Ed.* **2010**, *49*, 8033. (b) Bhugun, I.; Lexa, D.; Saveant, J.-M. *J. Am. Chem. Soc.* **1996**, *118*, 3982. (c) Rose, M. J.; Gray, H. B. *J. Am. Chem. Soc.* **2012**, *134*, 8310.

(6) Liu, T.; Wang, X.; Hoffmann, C.; DuBois, D. L.; Bullock, R. M. *Angew. Chem., Int. Ed.* **2014**, *53*, 5300−5304. Liu, T.; DuBois, D. L.; Bullock, R. M. *Nat. Chem.* **2013**, *5*, 228−233.

(7) (a) Nguyen, A. D.; Rail, M. D.; Shanmugam, M.; Fettinger, J. C.; Berben, L. A. *Inorg. Chem.* **2013**, *52*, 12847−12854. (b) Le Cloirec, A.; Davies, S. C.; Evans, D. J.; Hughes, D. L.; Pickett, C. J.; Best, S. P.; Borg, S. *Chem. Commun.* **1999**, 2285. (c) Singleton, M. L.; Reibenspies, J. H.; Darensbourg, M. Y. *J. Am. Chem. Soc.* **2010**, *132*, 8870. (d) Singleton, M. L.; Crouthers, D. J.; Duttweiler, R. P.; Reibenspeis, J. H.; Darensbourg, M. Y. *Inorg. Chem.* **2011**, *50*, 5015. (e) Quentel, F.; Passard, G.; Gloaguen, F. *Chem.—Eur. J.* **2012**, *18*, 13473.

(8) Connor, G. P.; Mayer, K. J.; Tribble, C. S.; McNamara, W. R. *Inorg. Chem.* **2014**, *53*, 5408−5410.

(9) (a) McQuilken, A. C.; Jiang, Y.; Siegler, M. A.; Goldberg, D. A. *J. Am. Chem. Soc.* **2012**, *134*, 8758−8761. (b) Noveron, J. C.; Olmstead, M. M.; Mashcharak, P. K. *J. Am. Chem. Soc.* **2001**, *123*, 3247. (c) Heinrich, L.; Li, Y.; Vaissermann, J.; Chottard, G.; Chottard, J.-C. *Angew. Chem., Int. Ed.* **1999**, *38*, 3526.

(10) Lee, Y.-M.; Hong, S.; Morimoto, Y.; Shin, W.; Fukuzumi, S.; Nam, W. *J. Am. Chem. Soc.* **2010**, *132*, 10668.

(11) (a) Roberts, J. A. S.; Bullock, R. M. *Inorg. Chem.* **2013**, *52*, 3823−3835. (b) Fourmond, V.; Jacques, P. A.; Fontecave, M.; Artero, V. *Inorg. Chem.* **2010**, *49*, 10338−10347.

(12) (a) Helm, M. L.; Stewart, M. P.; Bullock, R. M.; Rawkowski-Dubois, M.; Dubois, D. L. *Science* **2011**, *333*, 863.

(13) McCarthy, B. D.; Martin, D. J.; Rountree, E. J.; Ullman, A. C.; Dempsey, J. L. *Inorg. Chem.* **2014**, *53*, 8350−8361.

(14) Thapper, A.; Behrens, A.; Fryxelius, J.; Johansson, M. H.; Prestopino, F.; Czaun, M.; Rehder, D.; Nordlander, E. *Dalton Trans.* **2005**, 3566−3571.

DOI: 10.1021/ic5030394
Inorg. Chem. 2015, 54, 3325−3330